Theoretical and Experimental Comparison of Pressure in a Standing Wave Tube with Attenuation

John Nichols

Department of Physics, University of Illinois at Urbana-Champaign

ABSTRACT

In an attempt to have a controllable acoustical system that is completely understood in our lab, a rigidly-terminated standing wave tube is studied. Having a more complete understanding of the sound field inside this tube will allow future experiments to continue to build on this foundation of knowledge. Pressure and particle velocity measurements were made on both ends of the tube, to be compared with a method of images theory. The measurements agree with the theory to a great degree of accuracy and our awareness of what is happening inside the standing wave tube has increased.

Why Standing Wave Tubes?

Standing wave tubes (SWTs) are interesting to study because they are not too difficult conceptually, and they are an enclosed, controllable environment. SWTs are also relatively simple. Below a cutoff frequency, only plane waves can travel freely inside a SWT. That frequency is given by $f_{\text{cutoff}} = \frac{1.84 \cdot c}{\pi \cdot D}$, where c is the speed of sound and D is the diameter of the pipe.[1] This restriction means that a SWT below the cutoff frequency can be treated as a one dimensional object.

SWTs are used worldwide in acoustics for calibration and measurement purposes. For example, if a material needs to be tested with low frequency sound in free space, the dimensions of the sample should be large when compared to the acoustic wavelength. At 100 Hz, that means the dimensions of the sample would have to be more than 3.5 meters across, otherwise the sound can just bend around the sample. By placing this material in or at the end of a SWT, only a material as large as the cross-sectional area of the tube is required.

Currently, most acoustic reflection measurements of materials are made using standing wave tubes. This typically involves a SWT with a loudspeaker fully closing one end of the tube and the sample covering the other end. Then at two or three locations along the length of the tube, pressure and particle velocity measurements are made. Various other methods have been used, one of which involves manually sweeping the length of the tube with a microphone probe to find the pressure maxima and minima which can then be related to give a reflection factor. [2-3]

The setup and method used in this study is different from these methods in that the tube is rigidly terminated on both ends with only a small portion of one of the ends being the sound source, allowing for near total reflection at both ends of the tube.

Representing Attenuation with a Complex Wavenumber

In acoustics, complex acoustic pressure is the instantaneous deviation from atmospheric pressure. A propagating plane wave, with no dissipation, in the positive z-direction could be described by the following formula: $\tilde{P}(z,t) = P_0 \cdot e^{i(\omega t - kz)}$. Add to that an attenuation term that decays exponentially and the pressure becomes: $\tilde{P}(z,t) = P_0 \cdot e^{i(\omega t - kz)} \cdot e^{-\kappa z}$. This can be rewritten with a complex wavenumber as $\tilde{P}(z,t) = P_0 \cdot e^{i(\omega t - \tilde{k} z)}$, where $\tilde{k} = k - i\kappa$.[3]

Building and Calibrating P-U Microphones

At the beginning of the summer we started out by making cases and preamps for these tiny microphones. We laid out all the components on a small circuit board basing our design on previous mics used in the lab.[4] Each microphone box contains two transducers and two preamplifiers. The two transducers are a pressure condenser microphone and a differential pressure microphone. The circuit we assembled powers the transducers and does a little front end amplification and filtering. For the pressure microphone, the op-amp is set up for non-inverting 11× gain. For the differential pressure microphone, the op-amp is an integrator with 11× gain. The integral of differential pressure is proportional to the particle velocity, so the differential mic with an integrating op-amp is a particle velocity microphone. Once the circuit is completed, the microphones must be calibrated. The pressure (P) and particle velocity (U) outputs are individually connected to a voltmeter to measure the rms output voltage when the transducer is placed in a known sound field. This known sound field is a small calibration device that produces 1 kHz sound at 94 dB at a specific point inside the device. The tip of each transducer is placed at this point and the output voltage is measured.

Experimental Apparatus and Data Acquisition

The standing wave tube investigated is a stainless steel vacuum pipe that is 1.20 m in length and 6 cm inner diameter. See Fig. 1 and 2. The tube is held on a wooden stand which was placed on foam to acoustically isolate it from the table it was resting on. The tube is rigidly terminated at both ends with stainless steel blanks. A 1" hole is drilled in one of these blanks to house a piezoelectric transducer (PZT), which serves as the sound source. Another hole is drilled in each end to allow the P-U mics to be inserted into the ends of the tube. Complex pressure and particle velocity are measured using lock-in amplifiers (LIAs) in combination with the P-U mics. The outputs from the P-U mics are directed to the four LIAs which allows for simultaneous measurement of pressure and particle velocity at both ends of the tube. The PZT is driven by the function generator in one of the four LIAs used. This sine wave is also used as the

LIA reference signal. A computer saves the output from the LIAs.[5] Measurements were made in a 2 kHz window from 49.5 Hz to 2050.5 Hz in 0.1 Hz steps.

Figure 1. Left: Microphones inserted in one end of stainless steel tube. Right: Full experimental setup. Tube in foam on the table with lock-in amplifiers and computer under the table.

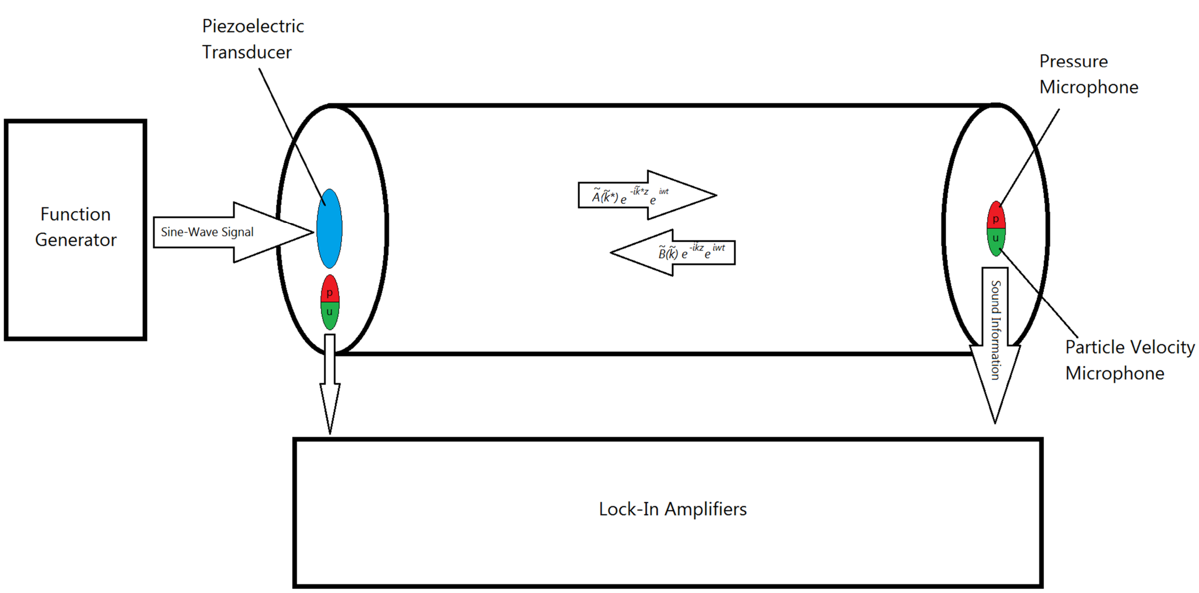

Figure 2. Schematic diagram of experimental setup. Piezoelectric transducer is excited by a sinusoidal signal to create a standing acoustic wave in the tube. Pressure and particle velocity are measured on each end of the tube. This data is analyzed by lock-in amplifiers.

Theoretical Model of a Standing Wave Tube

A standing wave is made up of two waves traveling in opposite directions. At any distinct point, the pressure would be the sum of these wave's pressures:

$$\tilde{P}(z,t) = \tilde{A}(\tilde{k})e^{i(\omega t - \tilde{k}z)} + \tilde{B}(\tilde{k})e^{i(\omega t + \tilde{k}z)},$$

where $\tilde{k}(\omega) = k(\omega) - i\kappa(\omega)$. Phase matching at the reflection boundary can be used to relate $\tilde{A}$ and $\tilde{B}$. Because there is no phase shift on reflection at the rigid end of the tube, $\varphi_A = \varphi_B$.

$$\varphi_A = \omega t - \tilde{k}z \qquad\qquad \varphi_B = \omega t + \tilde{k}z + \Delta\varphi$$

Setting $\varphi_A = \varphi_B$ at $z = L$,

$$\omega t - \tilde{k}L = \omega t + \tilde{k}L + \Delta\varphi$$

$$\text{So,} \qquad \Delta\varphi = -2\tilde{k}L, \qquad \text{and}$$

$$\tilde{B}(\tilde{k}) = \tilde{A}(\tilde{k}) \cdot e^{-2i\tilde{k}L}.$$ [1]

In order to solve for these coefficients, the method of images can be used to create an equivalent sound field to what is in the tube. This system is an infinite array of virtual sound sources at $z = 2nL$ where n is all integers. Each sound source has the same amplitude and all are driven in phase. Figure 3 illustrates how a virtual source at $z = 2L$ can model the same plane wave that would be seen as the first reflected wave. The instantaneous pressure at any point in the tube is a superposition of the pressure waves from this infinite array of virtual sources. This can be written as a summation:

$$\tilde{A}(\tilde{k}) = P_0 \sum_{n=0}^{\infty} e^{-2inkL} \cdot e^{-2n\kappa L} = \frac{1}{2}P_0\left[1 + \frac{\sinh(2\kappa L) - i\sin(2kL)}{\cosh(2\kappa L) - \cos(2kL)}\right].$$

Substituting for $\tilde{A}$ and $\tilde{B}$, the pressure becomes:

$$\tilde{P}(z,t) = \frac{1}{2}P_0\left[1 + \frac{\sinh(2\kappa L) - i\sin(2kL)}{\cosh(2\kappa L) - \cos(2kL)}\right] \cdot \left[e^{-i\tilde{k}z} + e^{i\tilde{k}(z-2L)}\right]e^{i\omega t}.$$

Looking at the Data

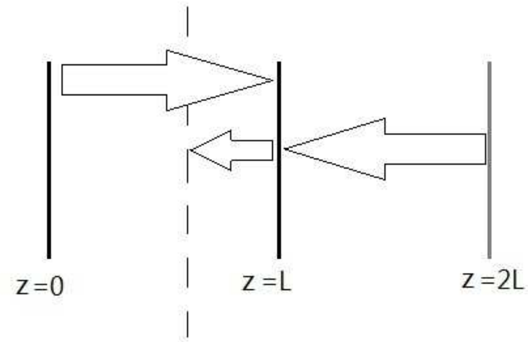

Figure 3. A sound originating at z=0 and reflecting back to a point in the tube can be modeled as starting at z=2L and travelling to the same point.

This experiment is intended to test and validate the theory of pressure in a SWT. Figure 4 presents the data collected at the end of the tube opposite the PZT. (a) shows the real component of pressure. It starts out negative with a sharp negative spike at the first resonance. The next resonance is an upward spike, alternating with each resonance. The amplitude of the spikes is fairly constant below 1500 Hz. Above this frequency, the amplitude increases rapidly. (b) shows the imaginary component of the pressure. This, too, starts out negative and has a downward spike at the first resonance, but instead of crossing zero between resonances, the zero-crossings and resonances coincide. The amplitude above 1500 Hz increases. (c) shows the pressure amplitude, ignoring phase. The resonant peaks are very clear. Between peaks, the dips do not go all the way down to zero; the minimum occurs slightly below 0.01 Pa. Like the real and imaginary components, the pressure amplitude increases by a factor of two between 1500 Hz and 2000 Hz. Lastly, (d) is a parametric plot of real vs. imaginary parts of the pressure. The graph is mostly horizontal with two lobes along the real axis. (e)-(h) show similar features, however, the amplitudes of the resonances are constant throughout the frequency range.

Figure 5 presents the pressure measurements on the source end of the tube, right next to the transducer. The real pressure, (a), is all positive getting to nearly zero between the resonances. The imaginary pressure, (b), looks almost like a tangent function, with a transition from maxima to minima at resonance, followed by a tangent-like curve back up to a maximum at the next resonance. The pressure amplitude, (c), looks very similar to (a), all positive with peaks at the resonances. The parametric plot, (d), only has one lobe in the positive real direction. (a)-(c) again show an increase in amplitude above 1500 Hz, while (e)-(h) share nearly all the same features but the increasing amplitude.

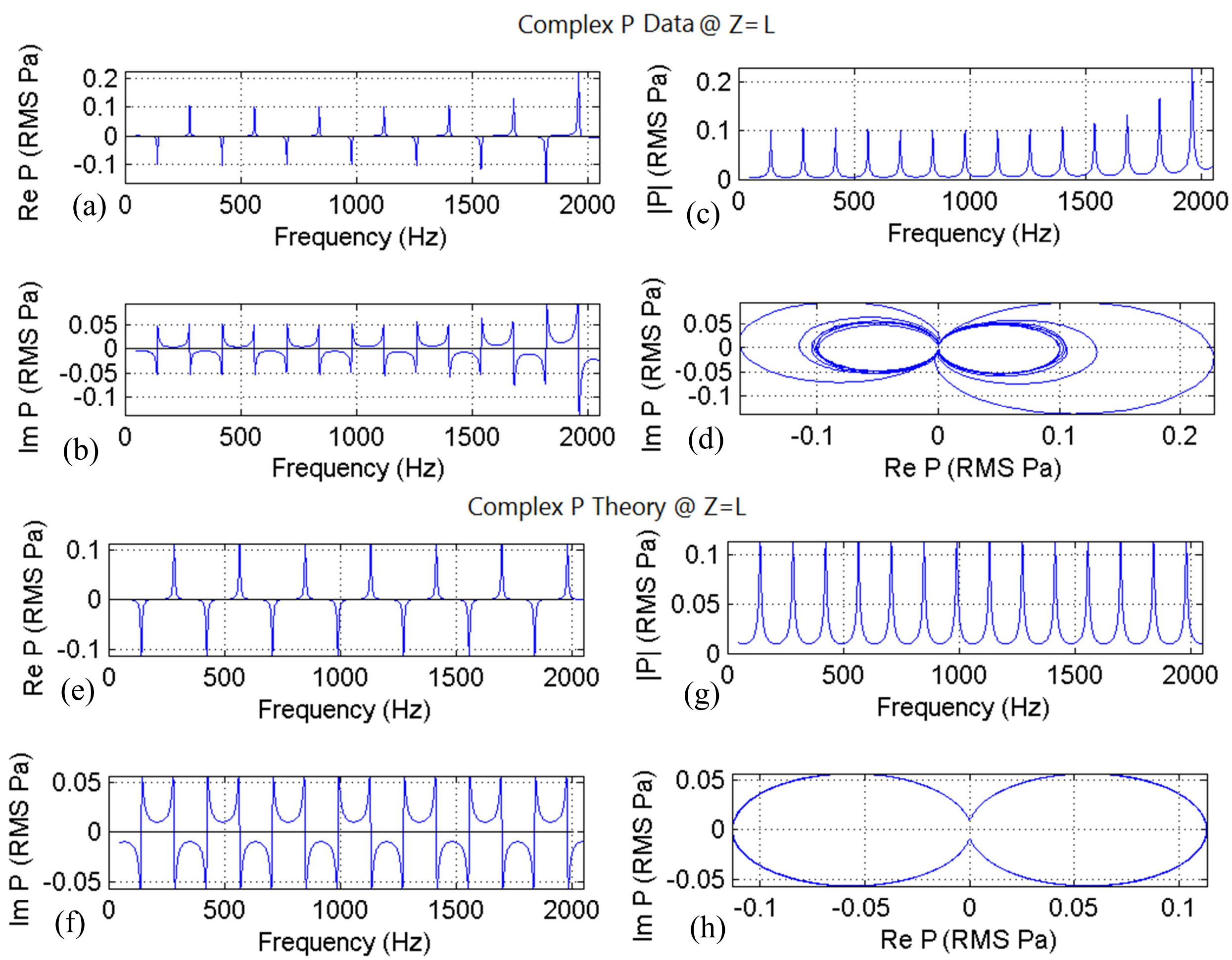

Figure 4. Complex pressure measurements at the far end of the SWT. (a)-(d) are experimental data. (e)-(h) are theoretical calculations. (a)&(e) are the real component of pressure. As expected, at the far end, the odd harmonics are out of phase with the PZT, while even harmonics are in phase. (b)&(f) are the imaginary pressure. (c)&(g) are the pressure amplitude. (d)&(h) are plots of the real vs. imaginary components of pressure. The increase in pressure as frequency increases in the measured data is attributable to a resonance in the PZT.

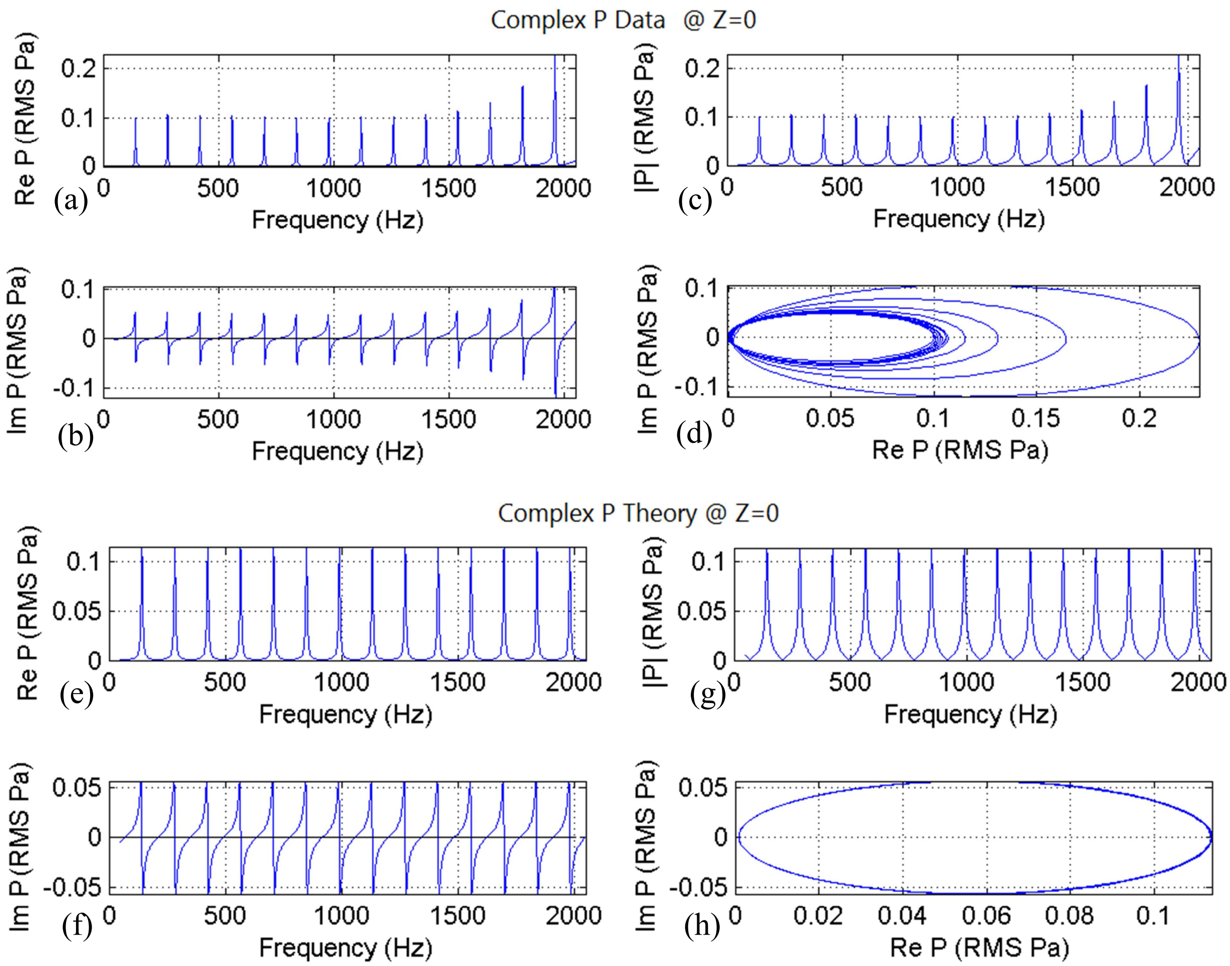

Figure 5. Complex pressure measurements at the source end of the SWT. (a)-(d) are experimental data. (e)-(h) are theoretical calculations. (a)&(e) are the real component of pressure. (b)&(f) are the imaginary pressure. (c)&(g) are the pressure amplitude. (d)&(h) are plots of the real vs. imaginary components of pressure. The increase in pressure as frequency increases in the measured data is attributable to a resonance in the PZT.

Comparing Theory to Experiment

Looking first at $z = L$ (Fig. 4), theory and experiment agree very well. In (a), real pressure at $z = L$ is out of phase with the driving signal for odd harmonics and in phase for even harmonics. This makes sense because when the tube resonates at the first harmonic, a half wavelength is present in the tube, whereas for even harmonics, having an integer number of wavelengths means the real part of pressure is in phase at both ends. In Figure 5(a), the real pressure is always in phase with the PZT. This is primarily because the pressure microphone is right in front of the sound source and should be in phase with it.

Another noteworthy feature of all of these graphs is that the resonant peaks have a finite width; they are not infinitely narrow peaks. This is due to dissipative effects present in the tube. The dissipative constant used in the theoretical calculations was chosen so that the resonant widths appeared to be about the same as in the data. This dissipative constant is highly dependent on atmospheric effects, especially humidity.

One large inconsistency remains when comparing theory and experiment, however. In the theory, peak amplitude remains constant across the frequency spectrum, while the measurements show an increasing amplitude above 1500 Hz. This seems to be because the signal frequency is approaching the first resonance of the piezoelectric driver, so the PZT can radiate a little more effectively, which manifests as a pressure amplitude increase.

Conclusions

Based on the comparison of theoretical calculations to experimental measurements, our theory of acoustic pressure in a standing wave tube with attenuation is believed to be correct. This means we are closer to fully understanding the sound field inside a standing wave tube. A more complete theory that includes particle velocity is being worked on. This theory could be generalized to have different boundary conditions at the ends of the tubes, possibly allowing for measurement of acoustic properties of exotic materials.

Acknowledgments

I would like to thank my advisor, Steven Errede, for sharing his expertise and guidance. I would also like to thank Laura Greene and Celia Elliott for their help and insight in Physics 496 & 499. This work was supported in part by the Anthony J. and Betty M. Anthony Summer Research Fellowship of the Department of Physics at the University of Illinois at Urbana-Champaign.

References

[1] S. M. Errede, *The Acoustical Physics of a Standing Wave Tube.* (Unpublished, 2011).

[2] M. G. Jones and T. L. Parrott, *Evaluation of a Multi-Point Method for Determining Acoustic Impedance.* Mech. Syst. Signal Pr. **3**(1), 15-35 (1989).

[3] L. Kinsler, A. Frey, A. Coppens, and J. Sanders, *Fundamentals of Acoustics, Fourth Edition.* (John Wiley & Sons, Inc., 1999).

[4] S. M. Errede, *Phys498POM Lecture 13.* UIUC Physics Dept, 2011. <http://online.physics.uiuc.edu/courses/phys498pom/498pom_lectures.html>.

[5] S. M. Errede, *Phys498POM Lecture 13 Part 2.* UIUC Physics Dept, 2011. <http://online.physics.uiuc.edu/courses/phys498pom/498pom_lectures.html>.